

The Mechanism of Regulation of Pantothenate Biosynthesis by the PanD–PanZ·AcCoA Complex Reveals an Additional Mode of Action for the Antimetabolite *N*-Pentyl Pantothenamide (N5-Pan)

Zoe L. P. Arnott,^{†,§} Shingo Nozaki,[‡] Diana C. F. Monteiro,^{†,§} Holly E. Morgan,[†] Arwen R. Pearson,[§] Hironori Niki,^{‡,||} and Michael E. Webb^{*,†,||}

[†]Astbury Centre for Structural Molecular Biology and School of Chemistry, University of Leeds, Leeds LS2 9JT, U.K.

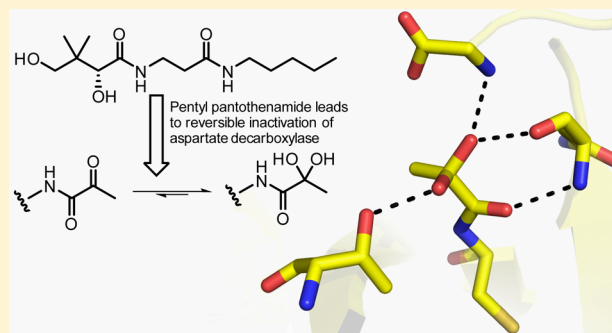
[‡]Microbial Genetics Laboratory, Genetics Strains Research Center, National Institute of Genetics, 1111 Yata, Mishima, Shizuoka 411-8540, Japan

[§]Hamburg Center for Ultrafast Imaging, Institute of Nanostructure and Solid State Physics, University of Hamburg, Luruper Chaussee 149, Hamburg 22761, Germany

^{||}Department of Genetics, Graduate University for Advanced Studies (Sokendai), 1111 Yata, Mishima, Shizuoka 411-8540, Japan

Supporting Information

ABSTRACT: The antimetabolite pentyl pantothenamide has broad spectrum antibiotic activity but exhibits enhanced activity against *Escherichia coli*. The PanDZ complex has been proposed to regulate the pantothenate biosynthetic pathway in *E. coli* by limiting the supply of β -alanine in response to coenzyme A concentration. We show that formation of such a complex between activated aspartate decarboxylase (PanD) and PanZ leads to sequestration of the pyruvoyl cofactor as a ketone hydrate and demonstrate that both PanZ overexpression-linked β -alanine auxotrophy and pentyl pantothenamide toxicity are due to formation of this complex. This both demonstrates that the PanDZ complex regulates pantothenate biosynthesis in a cellular context and validates the complex as a target for antibiotic development.



The antimetabolite pentyl pantothenamide **1** [NS-Pan (Scheme 1a)] was first described in 1970.¹ Like other pantothenamides, it has broad spectrum antibiotic activity but, uniquely, shows an order of magnitude improvement against *Escherichia coli*, with a minimum inhibitory concentration (MIC) of 2 $\mu\text{g mL}^{-1}$. Subsequent studies by Strauss and Begley demonstrated it is metabolized by three enzymes from the CoA biosynthesis pathway [pantothenate kinase (PanK), pantotheine adenylyltransferase (CoaD), and dephosphocoenzyme A kinase (CoaE)] to form ethyldethiacoenzyme A (EtdtCoA, **2**).² Remarkably, the *E. coli* metabolic enzymes favor the antimetabolite over the natural substrates by a factor of >10-fold. EtdtCoA is subsequently used as a substrate by phosphopantetheinyl transferases, forming inactive acyl carrier proteins (*crypto*-ACPs)³ as well as poisoning the cellular pool of coenzyme A. A similar mechanism of inhibition is observed in other bacteria, depending on the subtype of pantothenate kinase (PanK) present in the organism.⁴ Only promiscuous PanK_I and PanK_{II}-type enzymes that accept pantotheine as an alternative substrate to pantothenate are able to metabolize pentyl pantothenamide.⁵ PanK_{III}-encoding organisms are resistant to the antimetabolite.⁶ Formation of *crypto*-ACPs is not, however, the only source of toxicity in *E. coli*. Thomas and Cronan showed that *crypto*-ACPs can be effectively recycled by

the action of ACP hydrolase,⁷ and in the presence of an exogenous supply of pantothenate, the cells are rescued from growth inhibition. They therefore proposed that the toxic effects of pentyl pantothenamide were due to depletion of the cellular coenzyme A pool by an unknown additional mechanism.

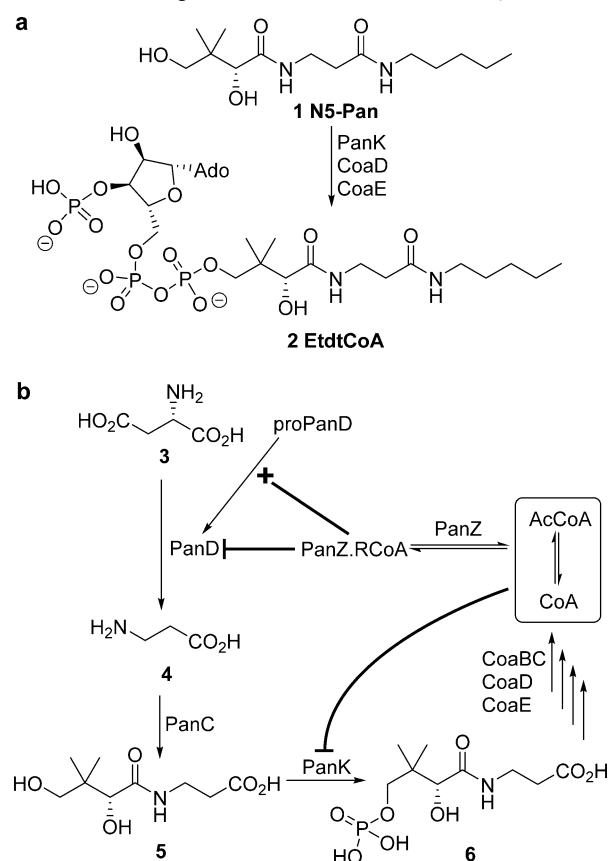
We have recently reported the structure of the complex formed between the zymogen of *E. coli* aspartate α -decarboxylase (proPanD) and its regulatory protein, PanZ.⁸ PanD is responsible for the production of β -alanine in the pantothenate biosynthesis pathway,⁹ and its catalytic action is dependent upon formation of a covalently bound pyruvoyl group from a serine residue via rearrangement of its peptide backbone.¹⁰ PanZ is required for the *in vivo* activation of *E. coli* proPanD, as the uncatalyzed rearrangement is too slow to support growth. PanZ is found in only a limited subset of enteric γ -proteobacteria, including the pathogens *Salmonella enterica*¹¹ and *Yersinia pestis*.¹² In those organisms that do not encode PanZ, such as *Mycobacterium tuberculosis*,¹³ it appears

Received: May 26, 2017

Revised: August 4, 2017

Published: August 23, 2017

Scheme 1. Relationship between Pentyl Pantothenamide (N5-Pan) and Regulation of Pantothenate Biosynthesis^a



^a(a) N5-Pan 1 is metabolized by PanK, CoaD, and CoaE to generate ethyl dethiacoenzyme A (EtdtCoA, 2). (b) Pathway from L-aspartate to coenzyme A. β-Alanine 4 is produced by decarboxylation of L-aspartate 3 by aspartate α-decarboxylase (PanD). β-Alanine then forms pantothenate 5, which is subsequently metabolized by PanK, CoaB, CoaC, CoaD, and CoaE to form coenzyme A 3. PanD is produced as a zymogen (proPanD) that is activated by the PanZ:RCoA complex but is also inhibited by the same complex.⁸ RCoA = AcCoA or CoA.

that the rearrangement is faster and autocatalytic. Our biophysical¹⁴ and structural⁸ characterization of the *E. coli* protein–protein complex revealed that the protein–protein interaction between PanZ and proPanD is dependent upon the presence of coenzyme A or acetyl-CoA (AcCoA). Following this observation, we demonstrated that PanZ has a second inhibitory role. While low-level expression of PanZ relieves the β-alanine auxotrophy caused by *panZ* deletion, overexpression of PanZ leads to inhibition of the pantothenate biosynthesis pathway due to inhibition of catalysis by activated PanD.⁸ At physiological concentrations of PanZ, we hypothesized that the protein–protein interaction provides a negative feedback mechanism for the pantothenate biosynthesis pathway in response to cellular CoA concentration (Scheme 1b). Given this regulatory mechanism, we investigated whether the enhanced toxicity of pentyl pantothenamide is due to accumulation of EtdtCoA, leading to downregulation of pantothenate biosynthesis mediated by this complex.

EXPERIMENTAL METHODS

Construction of Chromosomal *E. coli panD*(K119A) and Other Mutants. The 3.4 kb *ClaI*–*Sall* fragment

encompassing the *panD* gene from the chromosome of *E. coli* MG1655 was cloned into the *ClaI*–*Sall* site of pBR322 to construct pBR322*panD*. pBR322*panD* was digested with *ClaI*, and the consequent 5'-overhang was filled by the Klenow fragment of DNA polymerase I to form a blunt end; linearized pBR322*panD* was further digested by *Sall*. Similarly, pKH5002SB¹⁵ was digested with *XbaI* and the 5'-overhang filled by the Klenow fragment of PolI before being further digested by *Sall*. The *panD*-containing part of the *ClaI*(blunt)–*Sall* fragment from pBR322*panD* was cloned into the *XbaI*(blunt)–*Sall* site of pKH5002SB, resulting in pKH5002SB*panD*. The K119A mutation of *panD* [*panD*(K119A)] was introduced *in vitro* by overlap extension polymerase chain reaction (PCR)¹⁶ using primer sets of panDmutU and panD(K119A)L and of panD(K119A)U and panDmutL with pBR322*panD* as a template, to generate a 0.77 kb *NsiI*–*AflIII* fragment containing the *panD* gene. To construct pKH5002SB*panD*(K119A), the *NsiI*–*AflIII* fragment with the *panD*(K119A) mutation was exchanged with the corresponding wild-type fragment of pKH5002SB*panD*. pKH5002SB*panD*(K119A) was transformed into *E. coli* MG1655. Ampicillin-resistant clones, in which pKH5002SB*panD*(K119A) was integrated into the chromosome by homologous recombination, were obtained because the origin of the vector has a mutation such that the vector can be replicated only in *rnhA* mutant strains. pKH5002SB encodes the *sacB* gene of *Bacillus subtilis*, which is lethal to *E. coli* cells in the presence of sucrose. The transformants were therefore spread on sucrose-containing plates to select those colonies that lost the wild-type *panD* gene [or *panD*(K119A) gene] as well as the vector sequence by a second homologous recombination. The mutation was confirmed by PCR and DNA sequencing. *panD*(K14A), *panD*(K53A), and *panD*(K115A) were constructed using the same method, except that primers panD(K14A)U and panD(K14A)L, panD(K53A)U and panD(K53A)L, and panD(K115A)U and panD(K115A)L, respectively, were used (see the Supporting Information).

Construction of pBAD24*panZ* Mutants. The *panZ*(R73A) mutation was introduced *in vitro* by overlap extension PCR using primer sets of panZBADU40 and panZ(R73A)L and of panZ(R73A)U and panZL3 using MG1655 genomic DNA as a template. The PCR product was digested by *EcoRI* and *SphI* and cloned into the *EcoRI*–*SphI* sites of pBAD24. pBAD24*panZ*(R43A), pBAD24*panZ*(N45A), and pBAD24*panZ*(T72A) were constructed similarly using the primers listed in the Supporting Information.

Overexpression and Purification of Proteins. All proteins were overexpressed as described previously.^{8,12,17} For crystallization, PanD(WT) was overexpressed from vector pRSETA*panD* in *E. coli* C41(DE3) cells.¹⁷ For size-exclusion chromatography (SEC) analysis, PanD(WT) and PanD(K119A) were overexpressed from pET28*apanD* in *E. coli* Δ*panD* Δ*panZ* (DE3) cells.¹² For crystallization and isothermal titration calorimetry (ITC) analysis, PanZ(WT) was overexpressed using vector pET28*apanZ* in *E. coli* Δ*panD* Δ*panZ* (DE3) cells.⁸ For SEC analysis, PanZ(WT) was overexpressed using vector pBAD24*panZ* in *E. coli* Δ*panD* Δ*panZ* cells. For SEC and ITC analysis, PanZ(R73A) was overexpressed using pBAD24*panZ*(R73A) in *E. coli* Δ*panD* Δ*panZ* cells. All proteins were purified by sequential immobilized metal-affinity chromatography and SEC as described previously.⁸ CoaD and CoaE were overexpressed using the expression clones from the

Aska clones collection²⁶ and purified by single-step immobilized metal-affinity chromatography.

Crystallization and Structural Determination. For structural studies, the final SEC step for PanD and PanZ was performed via isocratic elution with Tris buffer [50 mM, 100 mM NaCl and 0.1 mM DTT (pH 7.5)]. The proteins were mixed in a 10:11 PanD:PanZ ratio (protomer to monomer) and concentrated to ~ 9 mg mL⁻¹ [Amicon centrifugal concentrator with a 10 kDa molecular weight cutoff (MWCO), 4500g], and 2 equiv of AcCoA were added.

Crystallization. Bipyramidal crystals were obtained using the hanging drop vapor diffusion method in 24-well plates. The protein was crystallized in 200 mM KSCN, 100 mM Bis-Tris propane (pH 6.5), and 20% (w/v) PEG 3350 at 18 °C. Crystal size varied depending on the protein:mother liquor ratios of the drops. Drops (3 μ L of protein + 1 μ L of mother liquor) gave the largest, best-diffracting crystals.

Data Collection. Crystals were cryoprotected stepwise in mother liquor containing 5, 10, and 20% (v/v) glycerol by soaking for a few seconds under each condition before being flash-cooled in liquid nitrogen. Diffraction data were collected at 100 K under a cryo-stream of dry nitrogen at beamline I03 (Diamond Light Source) at $\lambda = 0.9763$ Å; 900 frames of 0.2° oscillation, 0.1 s exposure, and 30% transmission were collected to a maximum resolution of 1.16 Å.

Data Reduction, Structure Solution, and Refinement. The data were integrated in space group I4 ($a = b = 85.9$ Å, $c = 80.1$ Å, and $\alpha = \beta = \gamma = 90^\circ$) using XDS.¹⁸ Data were scaled and merged in Aimless.¹⁹ The structure was determined by molecular replacement of the Protein Data Bank entry 4CRY model using Molrep²⁰ and iteratively manually rebuilt and refined with a mixed isotropic and anisotropic B factor model using Coot²¹ and Refmac5,²² respectively.

Isothermal Titration Calorimetry. All proteins for ITC were purified by SEC into 50 mM Tris, 100 mM NaCl, and 0.1 mM DTT (pH 7.4). Proteins were concentrated by centrifugal concentration (Amicon 10 kDa MWCO). Stock solutions of AcCoA were prepared at a concentration of 1 or 5 mM in gel filtration buffer and diluted to working concentrations using the flow-through from centrifugal concentration. Binding assays were performed by ITC using a Microcal iTC200 (GE) thermostated at 25 °C. The ligand sample was loaded into the sample cell (200 μ L), and the titrant was loaded into the sample syringe (70 μ L). Each titration experiment consisted of a sacrificial injection of 0.4 μ L followed by 19 injections of 2 μ L. Titration data were analyzed using NITPIC²³ and globally fitted in SEDPHAT.²⁴

Synthesis of *N*-Pentyl Pantothenamide (N5-Pan, 1) and Ethyldethiocoenzyme A (EtdtCoA, 2). Pentyl pantothenamide was synthesized via the route of Strauss and Begley² and purified by flash-column chromatography. EtdtCoA was generated via adaptation of literature procedures.^{2,25} *N*-Pentyl 4-dibenzylphosphopantothenamide was generated via phosphorylation of N5-Pan (1) using *N*-diethyl dibenzylphosphoramidate before deprotection by catalytic hydrogenation. EtdtCoA was generated via enzymatic turnover using CoaD and CoaE (overexpressed using constructs from the Aska clone collection²⁶) and purified by sequential reverse-phase HPLC and desalting steps. See the [Supporting Information](#) for the full synthetic procedures.

Growth Assay of *E. coli* Strains. For the assay on solid media, cell strains were grown to mid log phase in L or LB medium before being isolated by centrifugation, washed three

times with an equal volume of 1× M9 medium, and resuspended in the original volume of M9 medium. Cell optical density (600 nm) was used to quantify cell density prior to preparation of cell dilutions at OD₆₀₀ values of 0.01, 10⁻³, 10⁻⁴, 10⁻⁵, and 10⁻⁶. Samples (2 μ L) of each dilution were plated onto selective medium and grown for 45–48 h. For the continuous growth assay in liquid culture, exponentially growing cells in L medium were washed three times with M9 glucose minimal medium before dilution to a final density of 10⁻⁴ in 3 mL of defined growth medium, and cell growth was monitored using a Bio-Photorecorder TVS062CA (Advantec) with incubation at 37 °C. For end-point liquid culture assays, exponentially growing cells in 1% tryptone (or M9 glucose) at 37 °C were diluted to a final concentration of 10⁻⁴ in a total volume of 110 μ L and incubated overnight at 37 °C for 24 h.

RESULTS

Our previous studies of the system were focused on the mechanism of PanD activation, and we therefore determined the structure of an inactivatable PanD(T57V) site-directed mutant²⁷ bound to PanZ-AcCoA.²⁸ This structural analysis, together with independent evidence from both isothermal titration calorimetry and nuclear magnetic resonance (NMR), demonstrated that either coenzyme A or acetyl-coenzyme A was essential for the interaction of the pair of proteins. Binding of coenzyme A or its derivatives appears to structure the P loop of PanZ, enabling it to form a tight interaction with the C-terminal peptide of PanD(T57V). Our hypothesis that PanZ regulates PanD in addition to catalyzing conversion of proPanD to PanD was based upon two observations: inhibition of PanD activity *in vitro* by PanZ and β -alanine auxotrophy as a result of overexpression of PanZ. Addition of PanZ-AcCoA to a PanD activity assay showed a decrease in the PanD enzymatic activity in both NMR- and ITC-based assays. Confirmation of the regulatory mechanism in a cellular context requires additional proof. We must show that PanZ interacts with PanD in a CoA-dependent manner, that the CoA concentration controls this interaction in the cell, that the interaction between PanZ and PanD is required for growth inhibition, and that the mechanism occurs at native levels of protein expression.

Structural Characterization of the PanD–PanZ Complex. We initially used X-ray crystallography to confirm that the interaction of PanZ-AcCoA with the activated wild-type enzyme is the same as that with the zymogen and CoA-dependent. Partially activated PanD (purified from a *panZ*⁺ strain of *E. coli* and therefore isolated as a mixture of both the proPanD zymogen and the catalytically active PanD forms^{10a}) was mixed with PanZ-AcCoA in a 1:1 ratio. Crystals of the complex were obtained, and diffraction data were collected to 1.16 Å. The structure was determined by molecular replacement (see [Table 1](#)). The overall architecture of the protein complex is isostructural with that observed for the PanD(T57V)–PanZ complex (see [Figure S1](#)).⁸ Four molecules of PanZ bind symmetrically to each face of the PanD tetramer, and AcCoA structures the P-loop of PanZ enabling interaction with the C-terminus of PanD.⁸

A mixture of proPanD and PanD was used in crystallization trials, but the structure in the crystal is that of the fully activated PanD, consistent with activation by PanZ during the crystallization process. The electron density at the active site is, however, inconsistent with the presence of a pyruvoyl group as observed in the apoenzyme by Albert et al.^{10b} (see [Figure S2](#)). Instead, a tetrahedral structure is present, consistent with

Table 1. Crystallographic Processing and Refinement Statistics for the Wild-Type PanD–PanZ·AcCoA Complex^a

| | |
|--|------------------------|
| beamline | Diamond I03 |
| temperature | 100 K |
| space group | I4 |
| cell dimensions <i>a</i> , <i>b</i> , <i>c</i> (Å) | 85.9, 85.9, 80.1 |
| resolution (Å) | 29.28–1.16 (1.18–1.16) |
| <i>R</i> _{merge} (%) | 7.7 (56.7) |
| <i>R</i> _{p.l.m.} (%) | 5.4 (39.5) |
| <i>I</i> /σ <i>I</i> | 9.0 (2.1) |
| completeness (%) | 99.6 (93.7) |
| multiplicity | 5.1 (4.4) |
| | Refinement |
| PDB entry | 5LS7 |
| resolution (Å) | 29.28–1.16 (1.19–1.16) |
| no. of reflections | 99822 (6688) |
| no. of free reflections | 4966 (391) |
| <i>R</i> _{work} (%) | 11.3 (19.6) |
| <i>R</i> _{free} (%) | 13.7 (22.3) |
| no. of atoms | |
| protein | 2130 |
| ligand/ion | 82 |
| water | 294 |
| average <i>B</i> factor (Å ²) | |
| protein | 16.96 |
| ligand/ion | 19.04 |
| water | 31.69 |
| root-mean-square deviation | |
| bond lengths (Å) | 0.034 |
| bond angles (deg) | 2.85 |

^aNumbers in parentheses refer to data for the highest-resolution shell.

the presence of the (usually) thermodynamically disfavored ketone hydrate (Figure 1a). We repeated the structural elucidation using fully activated PanD. We observed the same structure using both room-temperature and cryo-cooled crystals (data not shown), indicating that the hydrate is formed from the pyruvoyl cofactor and is not an intermediate in the activation reaction. This state is stabilized by a hydrogen bond to the amide of Gly24, which is held in place by interactions with PanZ (Figure 1c). This suggests that binding of PanZ to the protein is able to generate specific changes in the microenvironment of the active site favoring this state. This provides a rationale for inhibition of catalysis by PanZ. To bind to the substrate, the protein–protein complex must first dissociate, allowing the pyruvoyl group to re-form; the substrate cannot bind at all in the presence of the inhibitory protein.

Overexpression-Linked Growth Inhibition Is Dependent upon CoA-Dependent Interaction of PanZ with PanD. The initial *in vivo* evidence of PanZ-induced inhibition of catalysis by ADC was that, while uninduced, leaky expression of PanZ leads to functional complementation of a Δ *panZ* strain of *E. coli*,¹² overexpression does not.⁸ We tested for this phenotype in the *panZ*⁺ *E. coli* MG1655 strain. Overexpression of PanZ restricts bacterial growth on minimal medium by inducing β -alanine auxotrophy (Figure 2a). It has previously been shown that *B. subtilis* ADC does not require PanZ for activation: an *E. coli* Δ *panD*::*BspanD* Δ *panZ* strain in which the *E. coli* ADC is replaced with the *Bacillus* protein is able to grow without β -alanine supplementation.¹² Furthermore, interaction of *E. coli* ADC and PanZ has been shown to be dependent upon interaction with a conserved C-terminal region of ADC,

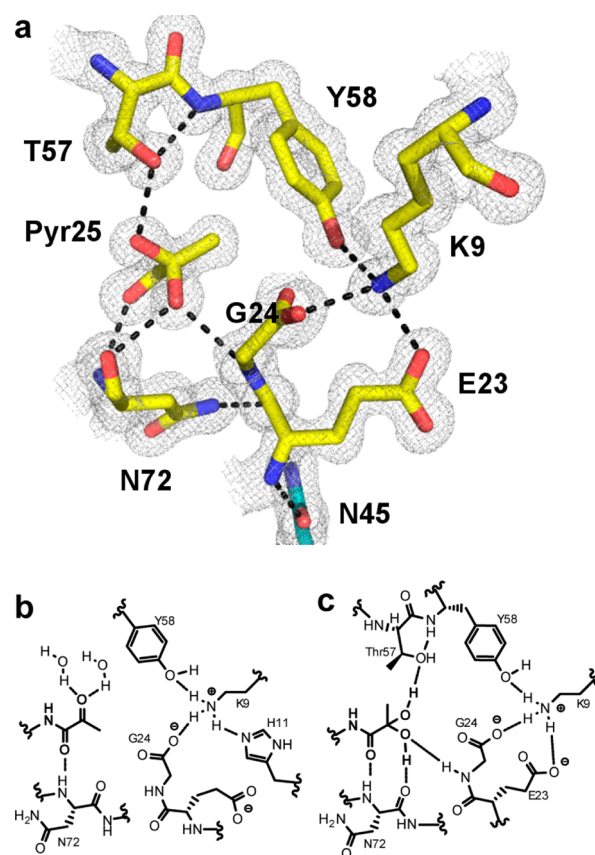


Figure 1. (a) Crystal structure of the PanZ·AcCoA–ADC complex at 1.16 Å resolution that reveals the pyruvoyl cofactor of activated ADC is present as a ketone hydrate in the complex. The $2F_o - F_c$ electron density is shown contoured at one rmsd as gray mesh. ADC carbons are colored yellow and PanZ carbons cyan (limited to residue N45, bottom); this figure was generated using PyMol. (b) Hydrogen bonding interactions in the vicinity of the pyruvoyl group in the apo state (PDB entry 1aw8^{10b}). The pyruvoyl keto group forms hydrogen bonds to solvent molecules. Residue K9 forms hydrogen bonds to Y58, H11, and the carboxylate of G24 (formed as a result of the activation reaction). (c) Hydrogen bonding interactions in the PanZ·AcCoA–ADC complex (PDB entry 5ls7, this work). A methyl-ketone hydrate form of the pyruvoyl cofactor is stabilized by hydrogen bonds to G24, T57, and N72. Binding of PanZ to the surface of PanD leads to formation of a hydrogen bond between N45 of PanZ and the backbone carbonyl of E23, distorting the hydrogen bonding network in the active site and displacing H11 from binding to K9.

deletion of which leads to loss of the protein–protein interaction.⁸ Because this region is not conserved in the *Bacillus* ADC, we anticipated that PanZ would not be able to interact with this protein and, consistent with this hypothesis, overexpression of PanZ does not lead to β -alanine auxotrophy in an *E. coli* Δ *panD*::*BspanD* strain (Figure 2a). This provides the first direct evidence that it is the physical interaction between PanD and PanZ that leads to growth arrest in *E. coli* as a result of PanZ overexpression.

The PanZ(N45A) mutant has previously been shown to be unable to complement a *panZ* deletion strain.¹² This is due to loss of a critical hydrogen bond (Figure 1a) that reduces the affinity between PanZ and proPanD from approximately 100 nM to 4 μ M, such that, at physiological concentrations of PanD and PanZ, the complex does not form.⁸ We therefore screened a range of site-directed mutants to identify any that could still complement the *panZ* deletion strain but were not susceptible

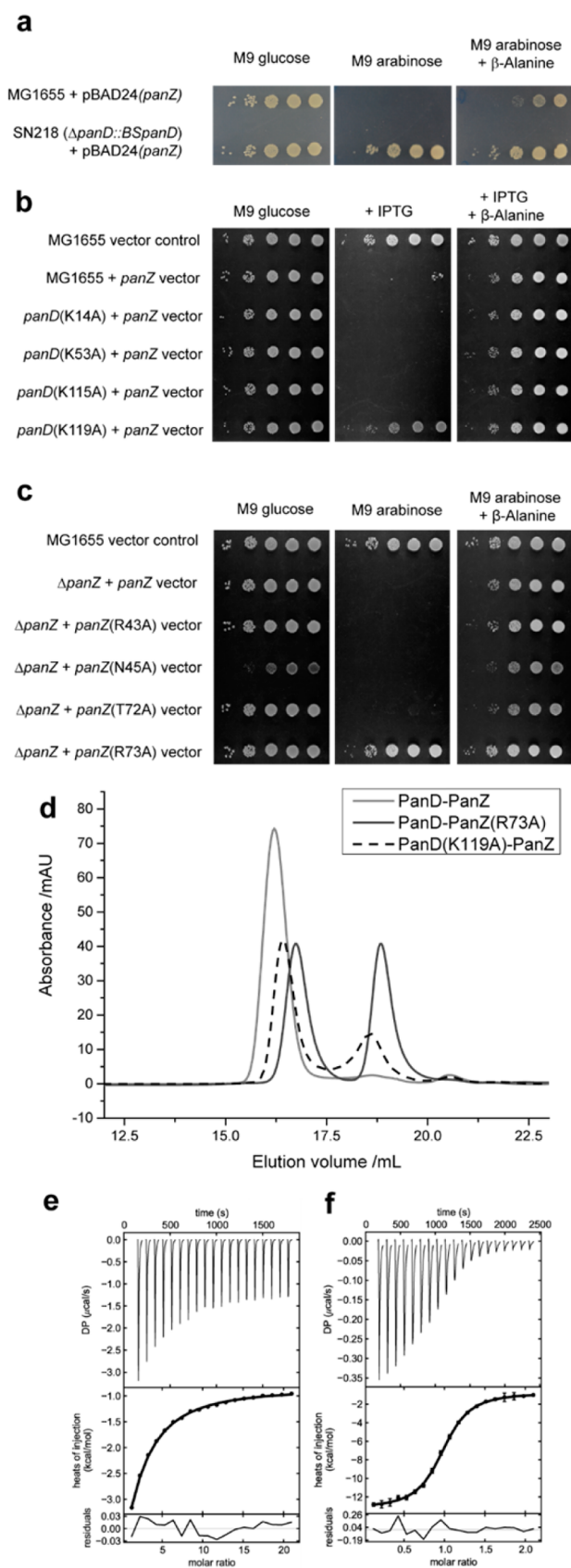


Figure 2. Regulation of ADC is due to CoA-dependent interaction of PanZ and ADC. (a) Overexpression of PanZ is sufficient to generate β -alanine auxotrophic bacteria. Growth of MG1655 is inhibited on M9 arabinose medium in the absence of β -alanine. In contrast, growth of

Figure 2. continued

strain SN218, in which the *panD* locus is replaced with that from *B. subtilis*, is not perturbed by PanZ overexpression. (b and c) Screening of mutations in panZ and panD to identify site-directed mutants that can relieve inhibition but maintain growth. (b) A K119A mutation in the chromosomal *panD* locus leads to loss of growth suppression. (c) Overexpression of panZ(R73A) does not inhibit cell growth. (d) Analysis of protein complex formation by SEC. The WT PanD–PanZ complex elutes as a heterooctamer (light gray line), whereas the PanD(K119A)–PanZ complex elutes as a mixture of the heterooctamer, PanD tetramer, and PanZ monomer (dashed line). The PanD–PanZ(R73A) mixture elutes as independent tetramer and monomer components (dark gray line). (e and f) Calorimetric analysis of interaction of PanZ(R73A) and AcCoA. (e) The loss of Arg73 from the AcCoA binding site reduces the affinity of the protein for AcCoA by ~250-fold. (f) Titration of PanZ(R73A) into PanD(S25A) in the presence of high concentrations of AcCoA (1 mM) indicates that the proteins interact at physiological concentrations of AcCoA.²⁹

to overexpression-induced growth inhibition. This screening process identified the site-directed mutants PanZ(R73A) and PanD(K119A) (Figure 2b,c). In both cases, the mutated protein still complements the β -alanine auxotrophy of the Δ *panZ* and Δ *panD* strains, indicating that catalytically active PanD is formed, but no growth inhibition is observed as a result of PanZ overexpression.

The effect of both mutations on complex formation was assessed *in vitro* using SEC of the purified proteins (see Figure 2d and Figure S3). While the wild-type PanD–PanZ complex elutes as a heterooctamer, the PanD(K119A)–PanZ complex eluted as a mixture of the heterooctamer complex and the individual proteins, suggesting a weakened protein–protein interaction. No heterooctamer could be observed for the PanD–PanZ(R73A) system, suggesting that these proteins do not form a stable complex. The fact that the PanZ(R73A) mutant can complement a Δ *panZ* strain, which requires activation of PanD, suggests the proteins must be able to interact to some extent. Residue Arg73 is involved in AcCoA binding by PanZ; the δ -guanidino group forms a salt bridge with Glu103, locking the pantetheine binding pocket (see Figure S4). For this mutant, we therefore reinvestigated the protein–protein interaction using ITC and the inactivatable PanD(S25A) mutant.²⁸ For PanZ(R73A), we observed a 250-fold change in the affinity for AcCoA { $220 \pm 30 \mu\text{M}$ [cf. $0.8 \mu\text{M}$ for WT PanZ (Figure 2d)]} but an only 6-fold decrease in the affinity for PanD in the presence of excess AcCoA (Figure 2e); global fitting yielded an estimate for this dissociation constant of $1.01 \pm 0.27 \mu\text{M}$, close to the previously determined affinity of 150 nM for WT PanZ for the S25A mutant.⁸ The reduced affinity for AcCoA is sufficient to account for the lack of an observed complex by SEC. Though the complex can form, it can accumulate only in the presence of high concentrations of AcCoA. This observation supports an AcCoA concentration-sensing role for PanZ; the reduced affinity for AcCoA means the inhibitory PanD–PanZ complex cannot accumulate at low concentrations of AcCoA.

High-Potency Growth Inhibition by Pentyl Pantothenamide Is Dependent upon the PanD–PanZ Interaction. Inhibition of growth as a result of overexpression may not be physiologically relevant as if the cellular concentration of PanZ is significantly lower than that of PanD then the inhibited complex may not accumulate. Both proteins have been detected via high-throughput proteomic abundance screening of *E. coli*,

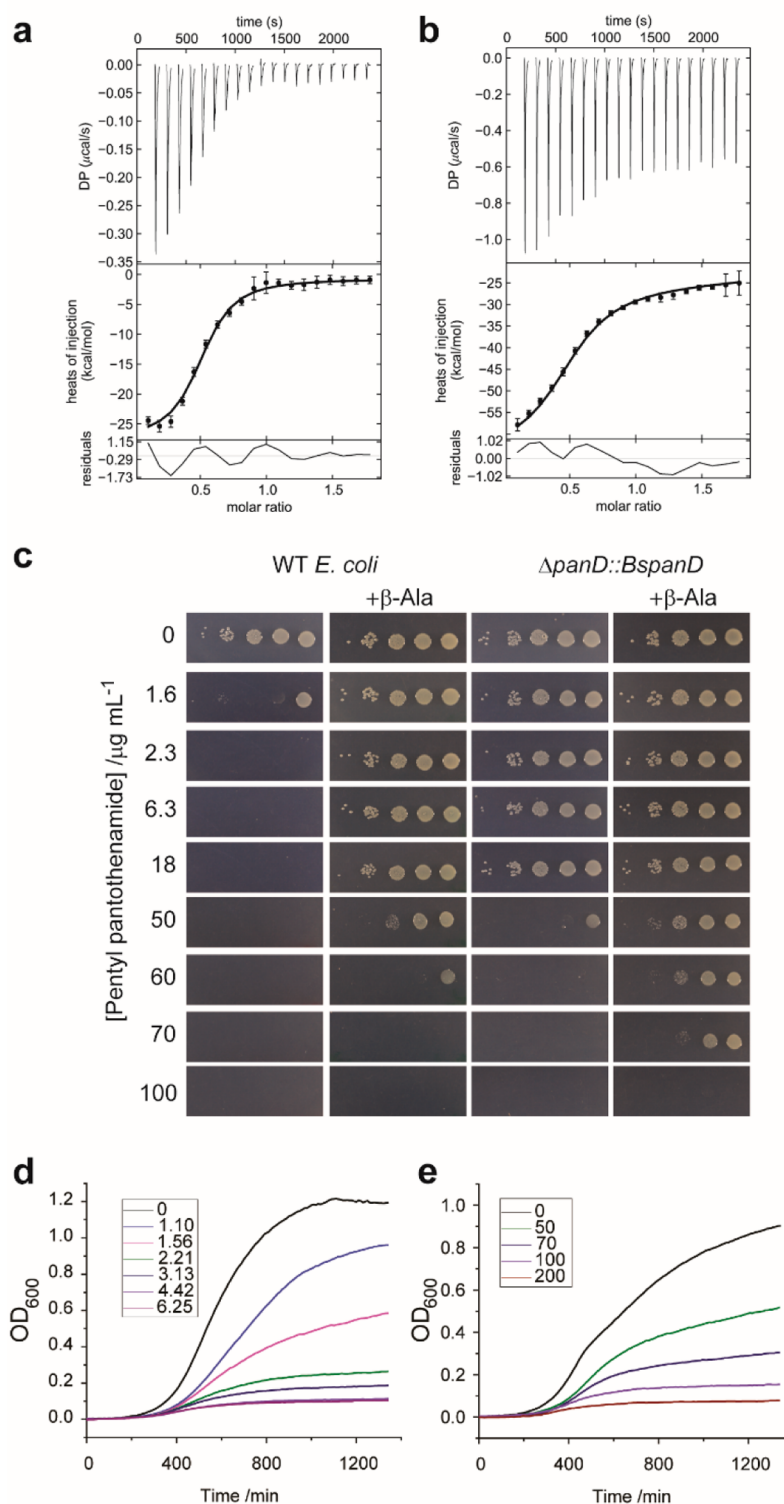


Figure 3. Testing of *E. coli* strains for growth inhibition by pentyl pantothenamide. (a) Titration of AcCoA against purified PanZ by ITC reveals substoichiometric but tight binding of AcCoA, due to co-purification of CoA with PanZ.¹⁴ (b) Binding of EtdtCoA to PanZ is indistinguishable from that of AcCoA [note the sloping baseline due to residual salt in the metabolite preparation (see Figure S5 for details of global fitting)]. (c) Growth of WT *E. coli* (MG1655) and a $\Delta\text{panD}::\text{BspanD}$ strain (SN218) on solid M9 agar medium supplemented with pentyl pantothenamide and β -alanine (0.5 mM). (d and e) Growth curves for MG1655 and SN218 ($\Delta\text{panD}::\text{BspanD}$), respectively, in liquid culture. Residual growth is observed even at inhibitory concentrations of the compound. (Inset – concentration of NS-Pan in $\mu\text{g mL}^{-1}$).

and these results suggest that the concentration of PanZ is slightly lower than that of PanD.³⁰ It is therefore possible that insufficient PanZ·CoA complex can form *in vivo* to markedly inhibit PanD. We therefore wished to use a small molecule

probe to investigate the behavior of the proteins at natural concentrations. Pentyl pantothenamide (NS-Pan) has previously been shown to exhibit enhanced activity against *E. coli* in comparison to other bacteria, as discussed above.^{1–3,7}

Because NS-Pan has been shown to be metabolized to ethyl dethiocoenzyme A (EtdtCoA) and downregulate CoA biosynthesis, we hypothesized that this effect was due to interaction of EtdtCoA with PanZ, resulting in subsequent inhibition of PanD. PanZ binds CoA and AcCoA with equal affinity, suggesting that PanZ will also bind EtdtCoA because PanZ is insensitive to modification of its ligand in this region. We therefore generated EtdtCoA by a combination of chemical synthesis to form *N*-pentyl phosphopantothenamide and enzymatic turnover using CoaD and CoaE to form the target molecule. We then used ITC to investigate binding of EtdtCoA to WT PanZ (Figure 3a). We observed tight binding, essentially indistinguishable from the signal observed for binding of AcCoA ($K_d = 524 \pm 64$ nM) to the same protein sample.

If EtdtCoA inhibits cell growth via the binding of the PanZ-EtdtCoA complex to ADC, a strain of *E. coli* in which PanZ and PanD cannot interact will be resistant; i.e., an *E. coli* SN218 ($\Delta panD::BspanD$) strain (which does not exhibit PanZ-mediated repression) should be resistant to pentyl pantothenamide. We therefore tested the activity of NS-Pan against both *E. coli* MG1655 and the *E. coli* SN218 strain. As expected, for MG1655, we observed a MIC of ~ 2 $\mu\text{g}/\text{mL}$, which increased to 50 $\mu\text{g}/\text{mL}$ with β -alanine supplementation (Figure 3b). For SN218, we observed a MIC of >50 $\mu\text{g}/\text{mL}$; in the presence of β -alanine, this increased to 100 $\mu\text{g}/\text{mL}$. Next, we investigated the inhibition of cell growth in liquid culture as a function of NS-Pan concentration (see Figure 3d,e and Figure S6). We observed a pattern of inhibition similar to that observed on solid medium, with inhibition of growth apparent at 4 $\mu\text{g}/\text{mL}$ for the WT strain. In contrast, 200 $\mu\text{g}/\text{mL}$ NS-Pan was required for full growth inhibition of the $\Delta panD::BspanD$ strain, with a profile similar to that seen for WT *E. coli* (MG1655) in the presence of β -alanine (see Figure S7a). This is fully consistent with NS-Pan acting by limiting the rate of pantothenate production; because the strain containing the *Bacillus* PanD is unregulated by PanZ, it is likely that this strain has a higher level of pantothenate production, enabling growth at the higher concentrations of NS-Pan.

In all cases, no change in the rate of cell growth is observed as a function of NS-Pan; instead, addition of NS-Pan restricts the final cell density in the stationary phase. Even at inhibitory levels of the compound, a small amount of residual growth is observed in direct proportion to the seeding density (see Figure S7b,c). If NS-Pan is inhibiting pantothenate biosynthesis, then this corresponds to growth on residual available pantothenate in the cells, indicating that the cell normally maintains a cellular pool of pantothenate and coenzyme A many times the minimal amount required for growth. Intriguingly, the maximal growth level also varies between the strains. A lower overall growth density is seen as a result of both β -alanine supplementation and substitution of the PanD (Figures S6 and S7a); this suggests that effective regulation of the coenzyme A biosynthetic pathway is critical to optimal cell growth.

DISCUSSION

In this work, we set out to confirm our original hypothesis, that binding of a PanZ-AcCoA complex to PanD regulates pantothenate biosynthesis *in vivo*.⁸ Almost all vitamin biosynthetic pathways in *E. coli* and other bacteria are tightly regulated, and numerous mechanisms for this regulation have been identified over the past 40–50 years. These include feedback allosteric regulation activity of pantothenate kinase activity in the pathway from pantothenate to coenzyme A,³¹

DNA binding transcription factors such as NadR that controls NAD biosynthesis,³² and metabolite binding riboswitches that control numerous pathways, including those for thiamine and cobalamin.³³ The consensus for the pantothenate biosynthetic pathway was that it is not regulated;³⁴ however, we recently proposed that the production of β -alanine is feedback-regulated by the PanZ-AcCoA complex.⁸ Our evidence for regulation was based on the overexpression phenotype of *panZ* and the *in vitro* inhibition of catalysis. To show that this inhibition is physiologically relevant, we needed to demonstrate both that growth inhibition was due to the CoA-dependent PanD–PanZ interaction and that the inhibition occurred at native concentrations of PanD and PanZ in the cell. The first point is demonstrated here by two observations. First, the PanD–PanZ interaction is the one required for the overexpression phenotype; substitution of the *E. coli panD* for the non-interacting *Bacillus panD* suppresses the phenotype. Second, a site-directed mutant of PanZ with reduced affinity for CoA no longer elicits the overexpression phenotype, indicating that CoA binding by PanZ is required for inhibition. Demonstration of inhibition in the absence of overexpression was achieved using the compound NS-Pan;¹ its rapid metabolism to form EtdtCoA in the cell² provides a pool of a ligand for PanZ that would engage this regulatory pathway. The observation that $\Delta panD::BspanD$ cells are resistant to the compound therefore supports our hypotheses that the PanD–PanZ complex is a target for the metabolites of NS-Pan and that the complex can act in a regulatory fashion *in vivo*.

The crystal structure of the PanD–PanZ complex unexpectedly revealed a methyl ketone hydrate at the active site. This provides an additional mechanism for inhibition of catalytic activity. Even if the substrate, aspartate, were to bind noncovalently to the complex, it cannot directly react with this form of the cofactor to produce the Schiff base conjugate required for catalysis. This therefore provides an additional, kinetic barrier to substrate binding, allowing more effective inhibition even in the presence of the 4 mM aspartate²⁹ found in exponentially growing *E. coli* ($\sim 50K_m$).^{10a} We have previously hypothesized that PanZ was originally recruited to regulate catalytic activity during the evolution of the γ -proteobacteria;⁸ many of these organisms are commensal organisms that grow in nutritionally rich environments in which pantothenate biosynthesis is dispensable. We suggest that a point mutation (or mutations) in the target protein, PanD, that enhances the affinity of the regulatory interaction may have inadvertently led to an absolute requirement for the interaction for conversion of proPanD to PanD to occur. This remains speculation, however, because no organism containing PanZ that does not also require it for activation has been identified.³⁵

The final finding in this work, that the enhanced activity of pentyl pantothenamide against *E. coli* is due to binding to PanZ, creates an opportunity to target this regulatory mechanism for antibiotic chemotherapy. What is the origin of this specificity? A vast array of pantothenamides have been synthesized and tested, yet none have matched the potency of NS-Pan for inhibition of *E. coli* growth.^{4,36} The binding of PanZ to AcCoA, the binding of PanZ to CoA, and the binding of PanZ to EtdtCoA are essentially indistinguishable, and the structure of the acetyl binding pocket supports this observation; no specific hydrogen bonding interactions involve the acetyl group of AcCoA, suggesting that loss of the carbonyl group will not lead to loss of binding affinity. The methyl of the acetyl moiety binds in a shallow pocket that can therefore readily

accommodate the terminal methyl group of EtdtCoA. However, it may not be able to accommodate longer analogues, suggesting a rationale for the loss of activity in the series going from NS-Pan to *N*-heptyl pantothenamide. Because CoA binds with equal potency, it appears that this binding pocket has little effect on the binding, and we would therefore have expected shorter homologues, e.g., methyldeithiacoenzyme A or deithiacoenzyme A, to bind equally well. The fact that the antimetabolites *N*-butyl pantothenamide and *N*-propyl pantothenamide are less active, despite being substrates for *E. coli* PanK,⁴ suggests that binding to PanZ is compromised or their metabolism in the cell by CoaD and CoaE is less effective. In any case, our structural model provides an opportunity to identify new more potent inhibitors of this biosynthetic pathway via rational design and experimentation.

CONCLUSION

In conclusion, we have demonstrated that growth inhibition as a result of PanZ overexpression is linked to physiologically relevant regulation by the PanDZ complex of the pantothenate biosynthetic pathway in a cellular context. This demonstration was dependent upon the identification of the PanDZ complex as a target for the antimetabolite precursor pentyl pantothenamide (NS-Pan), providing the opportunity for structure-led design of novel compounds against this biosynthetic pathway.

ASSOCIATED CONTENT

Supporting Information

The Supporting Information is available free of charge on the ACS Publications website at DOI: 10.1021/acs.biochem.7b00509.

Supplementary figures, further details of ITC data analysis, size-exclusion chromatography, full protocols for small molecule synthesis, and associated analytical data (PDF)

AUTHOR INFORMATION

Corresponding Author

*E-mail: m.e.webb@leeds.ac.uk.

ORCID

Michael E. Webb: 0000-0003-3574-4686

Author Contributions

M.E.W., S.N., and H.N. conceived the project. S.N. constructed mutant strains and conducted growth assays and size-exclusion analysis. Z.L.P.A. synthesized pentyl pantothenamide and ethyl deithiacoenzyme A, purified proteins, and conducted ITC analysis. H.E.M. synthesized ethyl deithiacoenzyme A and conducted initial ITC analysis. D.C.F.M. and A.R.P. performed structural analysis of the WT PanD–PanZ complex. M.E.W. analyzed biophysical data, conducted growth assays, and wrote the paper. All authors contributed to revision of the manuscript. Z.L.P.A. and S.N. contributed equally to this study.

Funding

Z.L.P.A. is supported by a University of Leeds 110 Anniversary Scholarship and the University of Hamburg. D.C.F.M. was funded by a studentship from the Wellcome Trust (096684/Z/11/Z). M.E.W. was funded by the Wellcome Trust Institutional Strategic Support Fund (105615/Z/14/Z). A.R.P. is supported by the German Federal Excellence Cluster “The Hamburg Centre for Ultrafast Imaging”. Biophysical and structural analysis equipment was funded by the Wellcome Trust

(094232/Z/10/Z). We thank Diamond Light Source for access to beamline I03 (mx10305) that contributed to the results presented here.

Notes

The authors declare no competing financial interest.

ACKNOWLEDGMENTS

We acknowledge initial work on the production of ethyl deithiacoenzyme A by Reem Al-Shidani and technical assistance with ITC and NMR by Iain Manfield and Lars Kuhn, respectively.

ABBREVIATIONS

EtdtCoA, ethyldeithiacoenzyme A; NS-Pan, *N*-pentyl pantothenamide.

REFERENCES

- (1) Clifton, G., Bryant, S. R., and Skinner, C. G. (1970) *Arch. Biochem. Biophys.* 137, 523–528.
- (2) Strauss, E., and Begley, T. P. (2002) *J. Biol. Chem.* 277, 48205–48209.
- (3) Zhang, Y. M., Frank, M. W., Virga, K. G., Lee, R. E., Rock, C. O., and Jackowski, S. (2004) *J. Biol. Chem.* 279, 50969–50975.
- (4) de Villiers, M., Barnard, L., Koekemoer, L., Snoep, J. L., and Strauss, E. (2014) *FEBS J.* 281, 4731–4753.
- (5) Strauss, E., de Villiers, M., and Rootman, I. (2010) *ChemCatChem* 2, 929–937.
- (6) (a) Brand, L. A., and Strauss, E. (2005) *J. Biol. Chem.* 280, 20185–20188. (b) Hong, B. S., Yun, M. K., Zhang, Y.-M., Chohnan, S., Rock, C. O., White, S. W., Jackowski, S., Park, H.-W., and Leonardi, R. (2006) *Structure* 14, 1251–1261.
- (7) Thomas, J., and Cronan, J. E. (2010) *Antimicrob. Agents Chemother.* 54, 1374–1377.
- (8) Monteiro, D. C. F., Patel, V., Bartlett, C. P., Nozaki, S., Grant, T. D., Gowdy, J. A., Thompson, G. S., Kalverda, A. P., Snell, E. H., Niki, H., Pearson, A. R., and Webb, M. E. (2015) *Chem. Biol.* 22, 492–503.
- (9) Webb, M. E., Smith, A. G., and Abell, C. (2004) *Nat. Prod. Rep.* 21, 695–721.
- (10) (a) Ramjee, M. K., Genschel, U., Abell, C., and Smith, A. G. (1997) *Biochem. J.* 323, 661–669. (b) Albert, A., Dhanaraj, V., Genschel, U., Khan, G. L., Ramjee, M. K., Pulido, R., Sibanda, B. L., von Delft, F., Witty, M., Blundell, T. L., Smith, A. G., and Abell, C. (1998) *Nat. Struct. Biol.* 5, 289–293.
- (11) (a) Stuecker, T. N., Hodge, K. M., and Escalante-Semerena, J. C. (2012) *Mol. Microbiol.* 84, 608–619. (b) Stuecker, T. N., Tucker, A. C., and Escalante-Semerena, J. C. (2012) *mBio* 3, e00158-12.
- (12) Nozaki, S., Webb, M. E., and Niki, H. (2012) *MicrobiologyOpen* 1, 298–310.
- (13) de Villiers, J., Koekemoer, L., and Strauss, E. (2010) *Chem. - Eur. J.* 16, 10030–10041.
- (14) Monteiro, D. C. F., Rugen, M. D., Shepherd, D., Nozaki, S., Niki, H., and Webb, M. E. (2012) *Biochem. Biophys. Res. Commun.* 426, 350–355.
- (15) Kitagawa, R., Ozaki, T., Moriya, S., and Ogawa, T. (1998) *Genes Dev.* 12, 3032–2043.
- (16) Sambrook, J., and Russell, D. W. (2001) *Molecular Cloning: A Laboratory Manual*, Cold Spring Harbor Laboratory Press, Plainview, NY.
- (17) Saldanha, S. A., Birch, L. M., Webb, M. E., Nabbs, B. K., von Delft, F., Smith, A. G., and Abell, C. (2001) *Chem. Commun.*, 1760–1761.
- (18) Kabsch, W. (2010) *Acta Crystallogr., Sect. D: Biol. Crystallogr.* 66, 125–132.
- (19) Evans, P. R., and Murshudov, G. N. (2013) *Acta Crystallogr., Sect. D: Biol. Crystallogr.* 69, 1204–1214.
- (20) Vagin, A., and Teplyakov, A. (2010) *Acta Crystallogr., Sect. D: Biol. Crystallogr.* 66, 22–25.

- (21) Emsley, P., Lohkamp, B., Scott, W. G., and Cowtan, K. (2010) *Acta Crystallogr., Sect. D: Biol. Crystallogr.* 66, 486–501.
- (22) Murshudov, G. N., Skubak, P., Lebedev, A. A., Pannu, N. S., Steiner, R. A., Nicholls, R. A., Winn, M. D., Long, F., and Vagin, A. A. (2011) *Acta Crystallogr., Sect. D: Biol. Crystallogr.* 67, 355–367.
- (23) Scheuermann, T. H., and Brautigam, C. A. (2015) *Methods* 76, 87–98.
- (24) Zhao, H., Piszczek, G., and Schuck, P. (2015) *Methods* 76, 137–148.
- (25) Tautz, L., and Retez, J. (2010) *Eur. J. Org. Chem.* 2010, 1728–1735.
- (26) Kitagawa, M., Ara, T., Arifuzzaman, M., Ioka-Nakamichi, T., Inamoto, E., Toyonaga, H., and Mori, H. (2006) *DNA Res.* 12, 291–299.
- (27) Webb, M. E., Yorke, B. A., Kershaw, T., Lovelock, S., Lobley, C. M. C., Kilkenny, M. L., Smith, A. G., Blundell, T. L., Pearson, A. R., and Abell, C. (2014) *Acta Crystallogr., Sect. D: Biol. Crystallogr.* 70, 1166–1172.
- (28) Schmitzberger, F., Kilkenny, M. L., Lobley, C. M. C., Webb, M. E., Vinkovic, M., Matak-Vinkovic, D., Witty, M., Chirgadze, D. Y., Smith, A. G., Abell, C., and Blundell, T. L. (2003) *EMBO J.* 22, 6193–6204.
- (29) Bennett, B. D., Kimball, E. H., Gao, M., Osterhout, R., Van Dien, S. J., and Rabinowitz, J. D. (2009) *Nat. Chem. Biol.* 5, 593–599.
- (30) Wang, M., Weiss, M., Simonovic, M., Haertinger, G., Schrimpf, S. P., Hengartner, M. O., and von Mering, C. (2012) *Mol. Cell. Proteomics* 11, 492–500.
- (31) (a) Rock, C. O., Park, H.-W., and Jackowski, S. (2003) *J. Bacteriol.* 185, 3410–3415. (b) Yun, M., Park, C.-G., Kim, J.-Y., Rock, C. O., Jackowski, S., and Park, H.-W. (2000) *J. Biol. Chem.* 275, 28093–28099.
- (32) Grose, J. H., Bergthorsson, U., and Roth, J. R. (2005) *J. Bacteriol.* 187, 2774–2782.
- (33) Winkler, W. C., and Breaker, R. R. (2005) *Annu. Rev. Microbiol.* 59, 487–517.
- (34) Cronan, J. E., Little, K. J., and Jackowski, S. (1982) *J. Bacteriol.* 149, 916–922.
- (35) Stuecker, T. N., Bramhacharya, S., Hodge-Hanson, K. M., Suen, G., and Escalante-Semerena, J. C. (2015) *BMC Res. Notes* 8, 354.
- (36) (a) Awuah, E., Ma, E., Hoegl, A., Vong, K., Habib, E., and Auclair, K. (2014) *Bioorg. Med. Chem.* 22, 3083–3090. (b) Virga, K. G., Zhang, Y. M., Leonardi, R., Ivey, R. A., Hevener, K., Park, H. W., Jackowski, S., Rock, C. O., and Lee, R. E. (2006) *Bioorg. Med. Chem.* 14, 1007–1020. (c) Mercer, A. C., Meier, J. L., Hur, G. H., Smith, A. R., and Burkart, M. D. (2008) *Bioorg. Med. Chem. Lett.* 18, 5991–5994.